ELSEVIER

Nuclear Instruments and Methods in Physics Research B 174 (2001) 297–303

NIM B
Beam Interactions with Materials & Atoms

www.elsevier.nl/locate/nimb

Hydrogen-related defect centers in float-zone and epitaxial n-type proton implanted silicon

P. Lévêque [a,*], P. Pellegrino [a], A. Hallén [a], B.G. Svensson [a,b], V. Privitera [c]

[a] *Royal Institute of Technology, Solid State Electronics, Electrum 229, 16440 Kista-Stockholm, SE, Sweden*
[b] *Department of Physics and Physical Electronics, Oslo University, P.B. 1048, Blindern, N-0316 Oslo, Norway*
[c] *CNR-IMETEM, Stradale Primosole 50, 95121 Catania, Italy*

Received 24 August 2000; received in revised form 12 October 2000

Abstract

Hydrogen-related defects in float zone (Fz) and epitaxial (Epi) n-type silicon crystals have been studied by means of deep level transient spectroscopy. These defects, as well as the characteristic vacancy-oxygen (VO) and divacancy (V_2) centers were introduced by proton implantation (1.3 MeV) using a dose of $1 \times 10^{10}/\text{cm}^2$. A hydrogen-related defect level located at 0.45 eV below the conduction band edge (E_c) appears in both kind of samples. Another hydrogen-related defect appears predominantly in the Fz samples with a level at $E_c - 0.32$ eV. Depth profiling as well as annealing studies strongly suggest that the level at $E_c - 0.45$ eV is due to a complex involving hydrogen and V_2. The level at $E_c - 0.32$ eV is strongly suppressed in the high purity Epi samples and the same holds for VO center. These results together with annealing data provide substantial evidence that the $E_c - 0.32$ eV level originates from a VO-center partly saturated with hydrogen (a VOH complex). Finally, in the Epi samples a new level at $\sim E_c - 0.31$ eV is resolved, which exhibits a concentration versus depth profile strongly confined to the damage peak region. The origin of this level is not known but the extremely narrow depth profile may indicate a higher-order defect of either vacancy or interstitial type.

PACS: 61.72.Cc; 61.72.Ji; 61.82.Fk; 61.72.Tt
Keywords: Defects; Ion implantation; Hydrogen; Silicon; DLTS

1. Introduction

High-energy proton implantation is a technique used for local control of the charge carrier lifetime in silicon power devices [1,2]. In comparison with the more conventional techniques used for lifetime control like gold diffusion or MeV electron irradiation, it offers the advantage of producing a non-uniform depth distribution of recombination centers. By using proton implantation, it is then possible to introduce deep levels in a reproducible way at a controlled depth in the active device region by varying the incident energy. During the

* Corresponding author. Tel.: +46-875-21126; fax: +46-875-27782.
E-mail address: leveque@ele.kth.se (P. Lévêque).

0168-583X/01/$ - see front matter
PII: S0168-583X(00)00524-3

last years, considerable efforts have been made to characterize the proton-induced defects. Even if progress has been achieved, the identity of the different hydrogen-induced defects is still controversial.

In this work the electron traps introduced by protons in high purity n-type float zone (Fz) and epitaxial (Epi) silicon have been studied by means of deep level transient spectroscopy (DLTS [3]). The hydrogen-related defects, as well as the characteristic vacancy-oxygen (VO) and divacancy (V_2) centers were introduced by proton implantation (1.3 MeV) using a dose of $1 \times 10^{10}/cm^2$. A hydrogen-related defect level located at 0.45 eV below the conduction band edge (E_c) appears in both kinds of samples. Another hydrogen-related defect appears predominantly in the Fz samples with a level at $E_c - 0.32$ eV. Annealing studies suggest strongly that the level at $E_c - 0.45$ eV is due to a V_2 center partly saturated with hydrogen. The level at $E_c - 0.32$ eV is almost suppressed in the oxygen lean Epi samples and the same holds for VO center. These results together with annealing data provide substantial evidence that the $E_c - 0.32$ eV level originates from a VOH complex. Finally, in the Epi samples a new level at $\sim E_c - 0.31$ eV is resolved, which exhibits a concentration versus depth profile strongly confined to the damage peak region. It is speculated that this level is due to a higher-order defect of intrinsic nature.

2. Experimental procedure

The samples used in this study were high purity Fz (1 0 0) Si and Epi layer Si of n-type (75 and 110 Ω cm, respectively). The Epi-layer (more than 50 μm thick) was grown by Molecular Beam Epitaxy on (1 0 0) silicon wafers. The proton (1.3 MeV) implantations were undertaken at The Svedberg Laboratory in Uppsala, where a beam line is equipped with an X–Y scanning facility for homogeneous area coverage [4]. The implantations were performed at room temperature (RT) with a constant dose of $1 \times 10^{10}/cm^2$. A 12 μm thick Al foil was placed at the surface of the wafers in order to have a mean projected range of ~12 μm according to transport of ions in matter (TRIM) calculations [5].

After implantation, the samples were chemically cleaned using a standard procedure which included a final dip in diluted hydrofluoric acid. Schottky barrier (SB) junctions were subsequently grown at low temperature (<40°C) by thermal evaporation of gold through a metal mask at a base pressure less than 2×10^{-6} Torr.

Analysis of the samples was performed by DLTS using an experimental setup described elsewhere [6]. Eight DLTS spectra with rate windows ranging from $(20\ ms)^{-1}$ to $(2560\ ms)^{-1}$ were simultaneously recorded during one single temperature scan from 77 to 300 K. The steady-state reverse bias and the filling pulse voltages were chosen to cover the whole defect profile. The filling pulse duration was 10 ms allowing to fully saturate traps with capture cross-sections as low as 10^{-18}–10^{-19} cm^2.

Concentration versus depth profiles were determined by selecting one of the eight rate windows and holding the temperature constant within ±0.5 K at the maximum of the DLTS peak of interest. The steady-state reverse bias voltage was kept constant while gradually increasing the majority carrier pulse. The depth profile was then extracted from the dependence of the DLTS signal on the pulse amplitude [3], where the voltages used were converted into depth by the conventional square-root dependence for an SB junction.

Isochronal annealing (30 min) of both types of implanted samples was performed in inert ambient (N_2).

3. Results and discussion

3.1. Defects monitored in Fz and Epi silicon after implantation

DLTS spectra for majority-carrier traps introduced in n-type Fz and Epi silicon samples by the proton implantation are shown in Fig. 1. Three characteristic traps are present in both types of implanted samples. They are well identified as follows: E_1, VO complex [7–9]; E_2, divacancy of doubly negative charge state (V_2^{2-}); E_4, divacancy

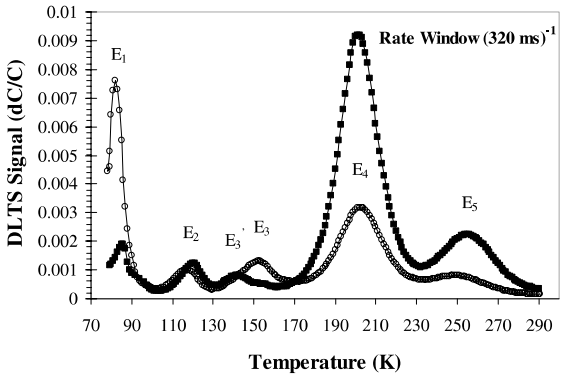

Fig. 1. DLTS spectra of Fz (open circles) and Epi (black squares) Si samples implanted at RT with a proton dose of $1 \times 10^{10}/\text{cm}^2$.

of singly negative charge state of V_2 (V_2^{1-}) [9–11]. E_4 is strongly overlapping with the vacancy-phosphorus defect (VP) as shown after subsequent annealing. Two other traps labeled E_3 and E_5 are present in the Fz sample. They have been identified previously as hydrogen-related traps [12,13]. Although much weaker, E_3 is also found in the Epi sample where also another trap (E_3') is clearly resolved. Simulations show that E_3 and E_3' are in fact present in both types of samples. E_3 dominates in the Fz sample while E_3' prevails in the Epi sample. Identification, energy position (below the conduction band edge E_c) and capture cross-section (σ) for the different traps as extracted from the experimental spectra by fitting simulations are displayed in Table 1.

As revealed by Fig. 1, the peak corresponding to VO is more intense in the Fz than in the Epi samples. This is expected because of the high purity Epi silicon with a lower interstitial oxygen concentration than in the Fz silicon. The hydrogen-related trap E_3 is also more intense in the Fz than in the Epi silicon (see Fig. 1), and these results support previous speculations that E_3 originates from a VO-center partly saturated with hydrogen (a VOH complex). Moreover, the level position found for this defect ($E_c - 0.32$ eV) is in agreement with the one extracted from Laplace DLTS measurements ($E_c - 0.31$ eV) and assigned to a VOH defect [14,15].

Concentration versus depth profile measurements have been performed for E_1, E_2, E_4 and E_5 in both types of samples and for E_3 in Fz and E_3' in Epi silicon, respectively. All the defect profiles are broader than the vacancy distribution as estimated by TRIM, except the E_3' profile that is rather narrow. Quantitatively, the average value of the full width at half maximum (FWHM) measured from the concentration profiles is only 1.6 μm for E_3' while it varies from 2 to 3.6 μm for the other traps. For comparison, the FWHM is 1.4 μm for the calculated vacancy concentration. This is illustrated in Fig. 2 where the concentration versus depth profiles of E_1 and E_3' in Epi silicon are displayed, as well as the calculated vacancy profile. It may indicate that E_3' is a high-order defect of either vacancy or interstitial type, possibly decorated by some impurity.

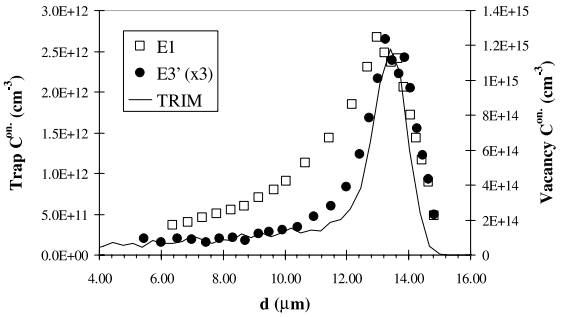

Fig. 2. Concentration versus depth profiles for E_1 and E_3' present in Epi (symbol) Si samples implanted with 1×10^{10} H^+/cm^2 and calculated vacancy distribution (line).

Table 1
Survey of the energy positions below E_c and electron capture cross-sections for the different traps (see labeling in Fig. 1).

Trap	E_1	E_2	E_3'	E_3	E_4	E_5
Energy (eV)	0.17	0.23	0.31	0.32	0.42	0.45
σ (10^{-14} cm^2)	~1	~0.1	~1	~0.3	~0.4	~0.005
Identification	VO	V_2^{2-}	?	H relat.	V_2^{1-} + VP	H relat.

Six pairs of samples (taken from the same wafer) of Fz and Epi silicon have been irradiated in parallel and an interesting statistical result is obtained: for each sample pair, the defect profiles are broader in the Fz than in the Epi silicon. It should be mentioned that for each pair of samples, they were simultaneously implanted using the same sample holder. This result is surprising and does not depend on some analysis artifact. Indeed, in high purity Epi silicon, less trapping of migrating vacancies and therefore a broadening of the defect profile as compared to Fz silicon is expected. In our case, the defect profiles are sharper but also deeper in the case of Epi silicon. This indicates strongly that ion-channeling takes place during the proton implantation despite a critical angle of only $\sim$0.3° [16] and the presence of the Al foil. Obviously, the channeling effect prevents a direct comparison between defect profiles measured in Fz and Epi silicon.

3.2. Annealing behavior of the monitored defects

DLTS spectra and concentration versus depth profiles have been recorded also after isochronal (30 min) annealing in inert ambient (N_2). All the defects studied in this part are observed after proton implantation with a dose of 1×10^{10} H^+/cm^2 and a dose rate of 3.3×10^9 H^+/cm^2 s. In Fig. 3 the depth profiles for E_4 in Epi silicon are compared before and after annealing at different temperatures. From these profiles, it is possible to calculate the integral concentration (or density) for each defect. Figs. 4 and 5 display the annealing behavior of E_2, E_4 and E_5 in Epi and Fz silicon, respectively.

The annealing behavior of E_4 shows two distinct steps with disappearance of the VP center at temperatures ranging from $\geqslant$ 100°C to 150°C in Epi and $\geqslant$ 70°C to 130°C in Fz silicon and the loss of V_2 above 230°C and 180°C in the Epi and Fz samples, respectively. Higher temperatures are required to anneal out VP and V_2 in Epi than in Fz silicon. This may be expected because of the low concentration of impurities in the Epi material and

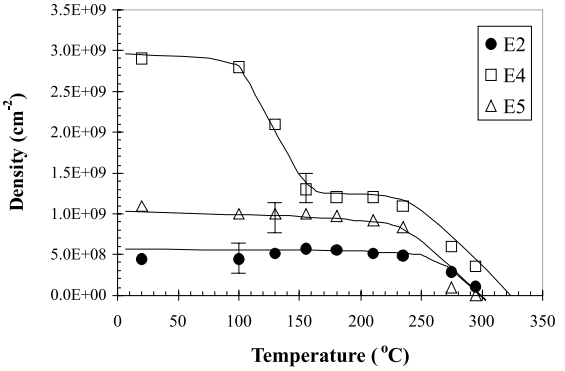

Fig. 4. Density of E_2, E_4 and E_5 in Epi silicon implanted with 1×10^{10} H^+/cm^2 and subsequently annealed at different temperatures. The solid lines are included to guide the eye.

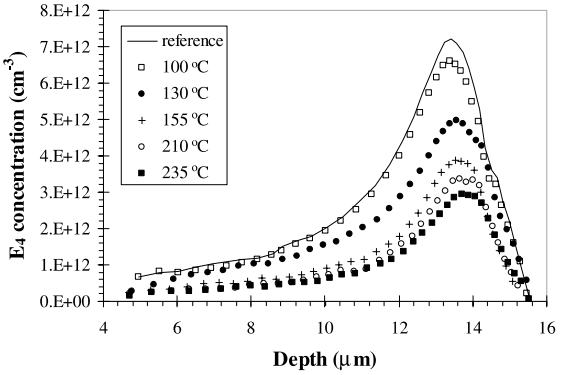

Fig. 3. Concentration versus depth profiles for E_4 in Epi silicon implanted with 1×10^{10} H^+/cm^2 and subsequently annealed at different temperatures.

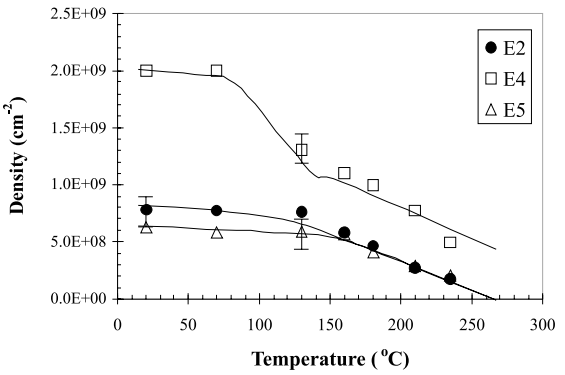

Fig. 5. Density of E_2, E_4 and E_5 in Fz silicon implanted with 1×10^{10} H^+/cm^2 and subsequently annealed at different temperatures. The solid lines are included to guide the eye.

is indicative of that long-distance migration of V_2 and VP prior to trapping and annihilation by impurities constitutes a major contribution to the annealing process [17]. From the first annealing step, it appears that the VP contribution in the E_4 trap is roughly 60% and 45% in Epi and Fz silicon, respectively. For the second annealing step, V_2 and E_5 exhibit the same behavior. E_5 has previously been shown to be hydrogen related because it does not appear after He implantation in Fz or Epi silicon. Its annealing behavior suggests strongly that E_5 is a complex involving hydrogen and V_2 with a breakup mechanism similar to that proposed for VOH^0 [18]. However, the concentration of E_5 does not correlate directly with that of V_2. Indeed, as shown in Figs. 4 and 5, the V_2 concentration is similar in both materials while the E_5 concentration is two times larger in Epi as compared to Fz silicon. On the other hand, the VO concentration is at least four times larger in Fz than in Epi silicon (this factor of four is a lower limit because VO is strongly overlapping with the C_iC_s pair in Epi silicon as shown below). By considering only the following set of equations:

$$VO + H \rightarrow VOH \quad (1a)$$

$$V_2 + nH \rightarrow V_2H_n \quad (1b)$$

it appears that the formation of V_2H_n (or E_5: reaction (1b)) will be favored in oxygen lean Epi silicon as compared to Fz silicon, even with similar V_2 concentrations. This simple argument shows only that the concentrations measured are not in contradiction with our identification of E_5.

E_3 is more stable than E_5 in Fz silicon and it does not anneal out before 250°C. This behavior suggests again that E_3 is a VOH complex, showing a thermal stability comparable to VO and greater than V_2 [18]. A previously suggested interpretation for E_3 formation (as a (H–V) defect [19]) is expressed by the following reaction:

$$(VP) + H \rightarrow (H\text{–}V) + P \quad (2)$$

From the annealing behavior of E_3, as illustrated in Fig. 6, it appears that there is no correlation between the loss of VP and the formation of E_3. The reaction described by Eq. (2) is, therefore, ruled out.

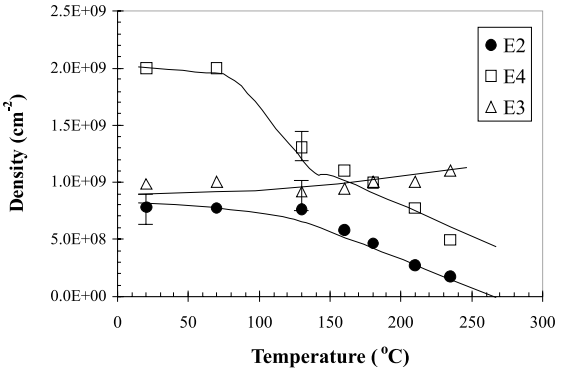

Fig. 6. Density of E_2, E_4 and E_3 in Fz silicon implanted with 1×10^{10} H^+/cm^2 and subsequently annealed at different temperatures. The solid lines are included to guide the eye.

As shown in Fig. 6, the E_3 concentration increases slightly as the V_2 concentration decreases. This has already been reported in the case of isothermal annealing of self-ion implanted Czochralski silicon [20]. The interpretation of Lalita et al. was that a limited supply of hydrogen gives rise to an increase of E_3 as a partly hydrogen saturated divacancy and at the same time to a decrease of V_2. Another possible explanation is that dissociation of V_2 increases the concentration of free vacancies that may be trapped by interstitial oxygen atoms, and subsequently, VOH complexes are formed in the case of a sufficient supply of migrating hydrogen atoms. This last explanation is consistent with our identification of E_3 and with its thermal stability.

E_3' is stable up to temperatures around 300°C and stays confined to a region as narrow as the calculated vacancy profile. This suggests again that E_3' may be a high-order defect of either vacancy or interstitial type, possibly decorated by some impurity. Theoretically, vacancy-clusters have been shown to be thermally more stable than V_2, for some special configurations like the hexavacancy (V_6) [21]. Nevertheless, no deep level is expected from V_6 and further work is needed to clearly identify E_3'.

In the Epi silicon, VO exhibits a reverse annealing behavior. Indeed, the density of E_1 increases as the annealing temperature increases as shown in Fig. 7. This increase appears while VP

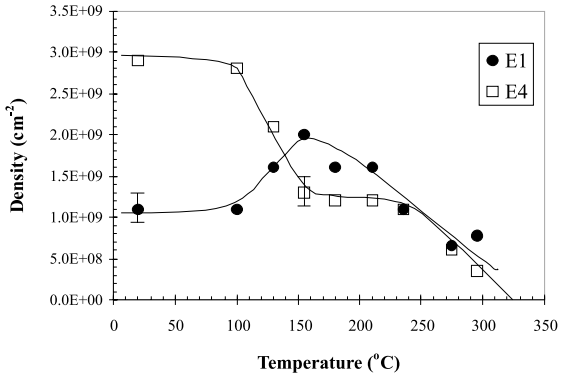

Fig. 7. Density of E_1 and E_4 in Epi silicon implanted with 1×10^{10} H^+/cm^2 and subsequently annealed at different temperatures. The solid lines are included to guide the eye.

anneals out. It can be due to the dissolution of VP that liberates vacancies that may be trapped by oxygen or to the formation of another defect (probably VP_2 [22]) strongly overlapping with the VO peak. By using DLTS filling pulse variations, it appears clearly that the first mechanism is dominating in our case. Indeed, DLTS pulse width variation measurements of E_1 show the two contributions of VO and of the C_iC_s pair (see Fig. 8), as expected for low oxygen content Epi silicon [23]. The first contribution, seen for pulses below $\sim$1 μs, corresponds to the VO capture rate while the other one is attributed to the C_iC_s pair [23]. The comparison of the DLTS filling pulse variations obtained before and after VP annealing (150°C, 30′) shows unambiguously that the VO contribution increases after VP annealing while the C_iC_s one remains constant. This observed increase in VO concentration is sufficient to explain the reverse annealing behavior found in Fig. 7 and fully supports the first mechanism described above.

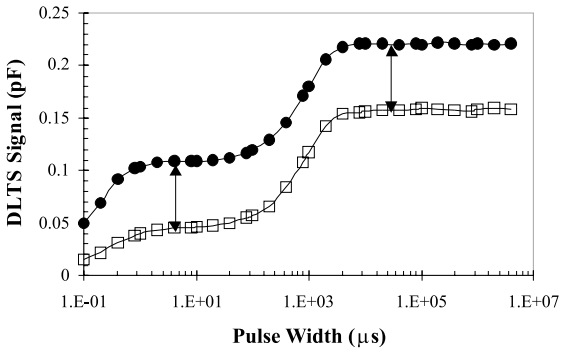

Fig. 8. DLTS pulse width variation of E_1 measured at 80 K in Epi silicon implanted with 1×10^{10} H^+/cm^2 before (open squares) and after (black circles) annealing of VP (150°C, 30′).

Finally, all the electrically active defects monitored during this study are passivated after an annealing at 330°C. The deactivation is presumably due to hydrogen stored in the sample after implantation while hydrogen contamination introduced, for example, during the cleaning procedure can be ruled out. Indeed, a piece of Fz and Epi implanted silicon has been annealed at 330°C before the cleaning procedure. SB junctions have been subsequently grown on these annealed samples and they exhibit exactly the same annealing behavior as the samples with the SB grown prior to annealing.

4. Conclusion

Three well-characterized deep levels are introduced in n-type silicon by low dose (1×10^{10} H^+/cm^2) high energy (1.3 MeV) proton implantation. They are identified as the VO complex, the divacancy of doubly negative charge state (V_2^{2-}) and singly negative charge state (V_2^{1-}), the latter one partially overlapping with the VP defect. Two-hydrogen-related levels are also resolved at 0.32 (E_3) and 0.45 eV (E_5) below the conduction band edge. E_3 appears predominantly in hydrogen implanted and oxygen-rich samples. Furthermore, it exhibits a similar annealing behavior as the VO defect and is assigned to a VOH complex. E_5 appears also only in hydrogen-implanted but not necessarily oxygen-rich samples. V_2 and E_5 exhibit a similar thermal stability and E_5 is identified as a complex involving V_2 and hydrogen. Another level (E_3') appears at 0.31 eV below the conduction band edge and is most clearly resolved in the Epi samples. Its narrow concentration versus depth profile indicates that E_3' may be a high-order defect of either vacancy or interstitial type, possibly decorated by some impurity.

Acknowledgements

We gratefully acknowledge support from the European Commission TMR Programme, network contract no. ERBFMRXCT 980228. Partial financial support was also received from the Swedish Research Council for Engineering Science (TFR).

References

[1] A. Mogro-Campero, R.P. Love, M.F. Chang, R.F. Dyer, IEEE Trans. Electron. Devices 33 (1986) 1667.
[2] D.C. Sawko, J. Bartko, IEEE Nucl. Sci. 30 (1983) 1756.
[3] D.V. Lang, J. Appl. Phys. 45 (1974) 3023.
[4] A. Hallén, P.A. Ingemarsson, P. Håkansson, G. Possnert, B.U.R. Sundqvist, Nucl. Instr. and Meth. B 36 (1989) 345.
[5] J.P. Biersack, L.G. Haggmark, Nucl. Instr. and Meth. 170 (1980) 208.
[6] B.G. Svensson, K.-H. Rydén, B.M.S. Lewerentz, J. Appl. Phys. 66 (1989) 1699.
[7] G.D. Watkins, J.W. Corbett, Phys. Rev. 121 (1961) 1001.
[8] J.W. Corbett, G.D. Watkins, R.M. Chrenko, R.S. McDonald, Phys. Rev. 121 (1961) 1015.
[9] L.C. Kimerling, in: N.B. Urli, J.W. Corbett (Eds.), Radiation Effects in Semiconductors, Inst. Phys. Conf. Ser., Vol. 31, 1977, p. 221.
[10] B.G. Svensson, M. Willander, J. Appl. Phys. 62 (1987) 2758.
[11] A.O. Evwaraye, E. Sun, J. Appl. Phys. 47 (1976) 3776.
[12] B.G. Svensson, A. Hallén, B.U.R. Sundqvist, Mater. Sci. Eng. B 4 (1989) 285.
[13] K. Irmscher, H. Klose, K. Maas, J. Phys. C: Solid State Phys. 17 (1984) 6317.
[14] A.R. Peaker, J.H. Evans-Freeman, P.Y.Y. Kan, L. Rubaldo, I.D. Hawkins, K.D. Vernon-Parry, L. Dobaczewski, Physica B 273–274 (1999) 243.
[15] K. Bonde Nielsen, L. Dobaczewski, K. Goscinski, R. Bendesen, Ole Andersen, B. Bech Nielsen, Physica B 273–274 (1999) 167.
[16] S.T. Picraux, J.U. Andersen, Phys. Rev. 186 (2) (1969) 267.
[17] P. Pellegrino, A.Yu. Kuznetsov, B.G. Svensson, Physica B 273–274 (1999) 489.
[18] P. Johannesen, B. Bech Nielsen, J.R. Byberg, Phys. Rev. B 61 (7) (2000) 4659.
[19] L. Palmetshofer, R. Reisinger, J. Appl. Phys. 72 (6) (1992) 2167.
[20] J. Lalita, B.G. Svensson, C. Jagadish, A. Hallén, Nucl. Instr. and Meth. B 127–128 (1997) 69.
[21] J.L. Hastings, S.K. Estreicher, P.A. Fedder, Phys. Rev. B 56 (16) (1997) 10215.
[22] A. Nylandsted Larsen, C. Christensen, J.W. Petersen, J. Appl. Phys. 86 (9) (1999) 4861.
[23] N. Keskitalo, A. Hallén, J. Lalita, B.G. Svensson, Mat. Res. Soc. Symp. Proc. 469 (1997) 233.